IEEE Access
Multidisciplinary | Rapid Review | Open Access Journal

Received September 17, 2019, accepted December 18, 2019, date of publication January 15, 2020, date of current version January 27, 2020.

Digital Object Identifier 10.1109/ACCESS.2020.2966716

Perspective Distortion Modeling for Image Measurements

ALEXANDRE BOUSAID, THEODOROS THEODORIDIS, SAMIA NEFTI-MEZIANI, AND STEVE DAVIS

Autonomous Systems and Advance Robotics Research Centre, SEE, University of Salford, Manchester M5 4WT, U.K.

Corresponding author: Theodoros Theodoridis (t.theodoridis@salford.ac.uk)

ABSTRACT A perspective distortion modelling for monocular view that is based on the fundamentals of perspective projection is presented in this work. Perspective projection is considered to be the most ideal and realistic model among others, which depicts image formation in monocular vision. There are many approaches trying to model and estimate the perspective effects in images. Some approaches try to learn and model the distortion parameters from a set of training data that work only for a predefined structure. None of the existing methods provide deep understanding of the nature of perspective problems. Perspective distortions, in fact, can be described by three different perspective effects. These effects are pose, distance and foreshortening. They are the cause of the aberrant appearance of object shapes in images. Understanding these phenomena have long been an interesting topic for artists, designers and scientists. In many cases, this problem has to be necessarily taken into consideration when dealing with image diagnostics, high and accurate image measurement, as well as accurate pose estimation from images. In this work, a perspective distortion model for every effect is developed while elaborating the nature of perspective effects. A distortion factor for every effect is derived, then followed by proposed methods, which allows extracting the true target pose and distance, and correcting image measurements.

INDEX TERMS Perspective distortion modeling, pose effect, distance effect, foreshortening effect, projective rotation, pose estimation, monocular vision.

I. INTRODUCTION

In perspective view everything changes like proportions, size, shapes, the angles that we see and even overlapped objects in the scene start to appear [1], [2]. The implication, out of perspective nature, results in the proposition of the perspective projection properties [3].

There are two types of distortions that can affect object shapes and sizes in a scene when projected into an image plane, which could lead to wrong image measurements [1], [4] (these two types of distortions are optical [5], [6]). The former is related to the design of the optical lenses [7], which plays an important role in bringing more light into the camera sensor. Lenses are way more complex [8]–[10] and the complexity of the lenses is beyond the scope of this paper. In this work, we focus on the latter type of distortion which has an important role in photography, image reconstruction, and image measurements.

The associate editor coordinating the review of this manuscript and approving it for publication was Senthil Kumar.

Perspective distortion refers to a state of spatial perception, where the state strictly depends on the position of the view-point with respect to the target objects within the scene. There are many sorts of perspective effects causing this aberrant appearance of the targets in the scene. Understanding these phenomena has long been an interesting topic for artists, designers and researchers, and various cases have to be taken into consideration; for example, in image diagnostic [11], monitoring [12], photogrammetry, object reconstruction [13], character reconstruction [14], [15] and pose estimation [16]–[18]. According to Aloimonos in [19], there are three different independent effects which describe perspective distortion. These effects refer to distance, position, and foreshortening. Because of distance effects, objects appear smaller as they move further away from the centre of projection. Position effects affect object shapes since angles are not preserved, but in fact they depend on the pose of the object. Finally, the foreshortening effect creates a shape distortion that depends on the angle formed by the line of sight from the centre of the object and the normal of the image plane [19].

All these facts and effects could lead to an eccentric error of the projected centre of the target in the image [20], [21]. This eccentricity is defined by the disparity of the true target centre projection onto the image and the centre of the projection in the image [22], [23]. Figure 1 illustrates the three forms of distortions of a target in the image.

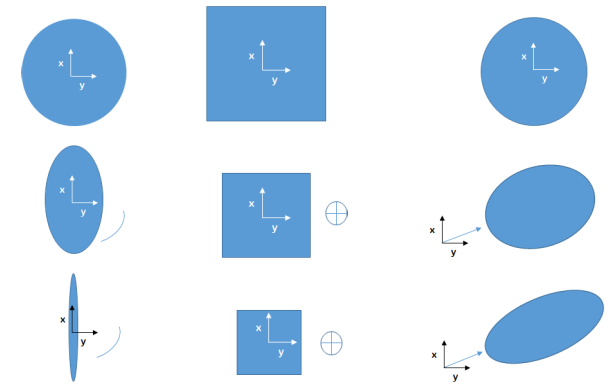

(a) Pose Effect (b) Distance Effect (c) Foreshortening Effect

FIGURE 1. Forms of perspective effects seen from the image plane.

Existing methods tried to model the perspective effect [24], some methods are based on the hypothesis constraints by the scene [25], like the position of the vanishing points within the image [26], or benefit from the stereo setup for adding up depth constraints to improve the model for measurements [27]. On the contrary, many other methods are based on learning patterns from a set of image data [13] like face recognition, ball tracking [28] and learning depth [29]–[31]. For every unique structure, a new data set is required and new training data are generated [13]. Existing methods for correcting the perspective effect from 2-Dimensional projective transformation using a popular geo-referencing techniques are being used worldwide [32]. All these methods do not provide any basic understanding of the nature of perspective problem. In this paper, we demonstrate novel models for every effect generated by perspective distortion, and provide clear understanding of the nature of the problem from a mathematical perspective, based on John Y. Aloimonos descriptions in [19]. Correction methods are then proposed and derived for different purposes. These models will serve as basic blocks for understanding the nature of perspective effects, extracting the true target pose and distance from its projected image data and correcting image measurements.

The second Section covers and studies the distortion effects on centred segments in space, providing mathematical derivation of the pose and distance factor. The third Section covers a foreshortening factor, which appears when segments are not centred. A mathematical derivation is depicted on the total distortion factor along with the derivation of the projective rotation model in 2D and 3D, and a mathematical derivation and analysis of finding the true centre on a line segment from its corresponding projected image. The fourth and fifth Sections cover proposed correction methods for image measurements. Finally, a summary, analysis and conclusion of the results achieved are discussed in Section six.

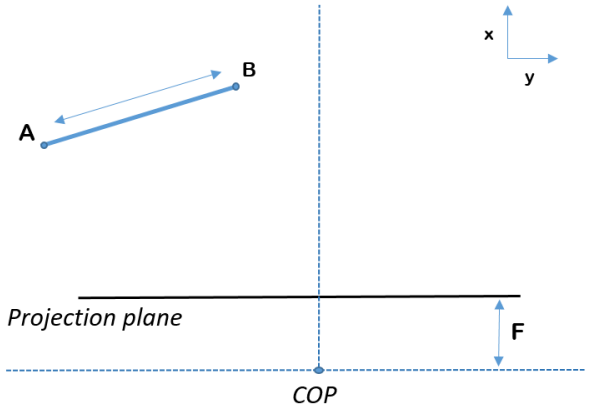

FIGURE 2. Line segment seen from a 2D perspective.

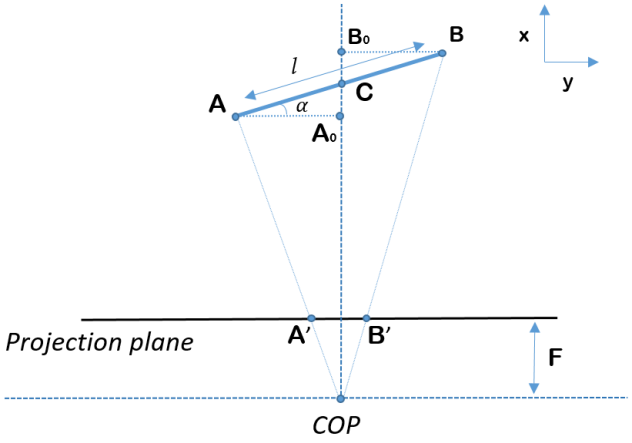

FIGURE 3. Centred line segment.

II. DISTORTION ON CENTRED TARGETS

For better understanding of the nature of these distortions, we extracted factors that model every distortion effect on segments since line segments form the basic blocks of any structure.

A line segment in an image is represented by its two end points $A = [x_A, y_A]^T$ and $B = [x_B, y_B]^T$, and of length l. Let $O(0, 0, 0)$ represent the COP of the view-point with focal distance f. For simplicity and good comprehension in this case, the segment is considered to be in a $2D$ space (XY) and thus the perspective plane, where the image is formed, is foreshortened to a line located at the focal distance F from the perspective view-point.

If the segment is placed to be coincident at its mid-point C that is perpendicular to the image plane and is tilted by an angle from this plane, the oblique projections of A and B towards the COP can be calculated from similarity and perspective projection that results (1) and (2). The projection of A and B are represented here by $A' = [x_{A'}, y_{A'}]^T$ and $B' = [x_{B'}, y_{B'}]^T$, simultaneously, and the tilted angle of the segment from the image plane is denoted by α.

For this particular case, where C is a midpoint and is coincident and perpendicular to the image plane, $x_C = (x_A + x_B)/2$, x_C becomes equivalent to the distance of the target from the COP. This leads to (3).

$$y_{A'} = \frac{F}{x_A} \cdot AC \cdot \cos(\alpha) \tag{1}$$

$$y_{B'} = -\frac{F}{x_B} \cdot BC \cdot \cos(\alpha) \tag{2}$$

$$x_C = \frac{F}{2} \cdot \left[\frac{y_{B'} - y_{A'}}{y_{B'} \cdot y_{A'}}\right] \cdot \frac{L}{2} \cdot \cos(\alpha) \tag{3}$$

$$\alpha = \arctan\left(\frac{F}{2} . \frac{y_{B'} + y_{A'}}{y_{A'} . y_{B'}}\right) \qquad \alpha \in [-\frac{\pi}{2} \ \frac{\pi}{2}] \tag{4}$$

Proof: From perspective projection $x_A = \frac{F}{y_{A'}} \cdot AC \cdot \cos\alpha$ and $x_B = -\frac{F}{y_{B'}} \cdot AC \cdot \cos\alpha$, in addition,

$$x_A - x_B = AB \cdot \sin\alpha$$

moreover

$$x_A - x_B = \left(\frac{F}{y_{A'}} + \frac{F}{y_{B'}}\right) \cdot AC \cdot \cos\alpha$$
$$= \left(F \cdot \frac{y_{B'} + y_{A'}}{y_{A'} \cdot y_{B'}}\right) \cdot AC \cdot \cos\alpha$$

which implies

$$AB \cdot \sin\alpha = \left(F \cdot \frac{y_{B'} + y_{A'}}{y_{A'} \cdot y_{B'}}\right) \cdot AC \cdot \cos\alpha$$

implies

$$\tan\alpha = \frac{F}{2} \cdot \left(\frac{y_{B'} + y_{A'}}{y_{A'} \cdot y_{B'}}\right)$$

implies

$$\alpha = \arctan\left(\frac{F}{2} \cdot \frac{y_{B'} + y_{A'}}{y_{A'} \cdot y_{B'}}\right)$$

□

A. DISTORTION FACTOR

Equations (1) and (2) show that the projection of any centred segment is dependent only on the segment distance x_C from the COP and the tilted angle α. We define our distortion factor to be the ratio of the projected length over the real length of the segment. We denote this factor by the small *mu* and is belonging to [0, 1]. Since the segment $[AB]$ is centred with respect to the COP we can write (5).

$$\mu = \frac{|y_{B'} - y_{A'}|}{L} \qquad \mu \in [0 \ 1] \tag{5}$$

B. POSE AND DISTANCE FACTORS

Replacing (1) and (2) in (5) yields to the following equation:

$$\mu = \underbrace{\left|\frac{4 \cdot x_C \cdot y_{B'} \cdot y_{A'}}{F \cdot L^2}\right|}_{\substack{\text{Distance} \\ \text{Distortion Factor}}} \cdot \underbrace{\left|\frac{1}{\cos(\alpha)}\right|}_{\substack{\text{Position} \\ \text{Distortion Factor}}} \tag{6}$$

The right hand side of (5) can be split into two factors where the right factor was named Distance Distortion factor (DDF) as μ_1, and the left factor was named Pose Distortion Factor (PDF) as μ_2. These two factors hold separate and independent information on how distance and pose affects our measurements in the image. It is clearly shown here that when $\alpha = 0$, meaning that the line lies in parallel to the image plane, the PDF is equal to one. In contrast, when X_C is equal to F, meaning that the target is located at the image plane, the DDF is equal to one. This yields to say that our μ factor is equal to one when no distortion is implied, and can be written as function of both distortions. However, since the segment $[AB]$ is centred, foreshortening distortion has no effect on the projection of $[A'B']$:

$$\mu = \mu_1 \cdot \mu_2 \tag{7}$$

In fact, as the centre of the segment moves away from the normal to the perspective plane, the foreshortening distortion starts appearing and provoking the projected length $[A'B']$ of the segment $[AB]$ to change non-linearly. In this case, μ has to hold for other factors due to the added foreshortening distortion to $[A'B']$, which we will see in the next section.

III. DISTORTION ON NON-CENTRED TARGETS

Considering a new segment represented by the points A and B, and of a mid-point C, to be placed anywhere in space. Since the centre of the target object, in this case the line segment, does not coincide with the focal axis, the projected image of the target is subject to additional distortion induced by the foreshortening effect. Modelling this effect requires to rotate the original segment back to the centre as shown in Figure 4. Within this context, this kind of rotation will be called projective rotation throughout the work, as we are rotating around the COP using only projected points as input.

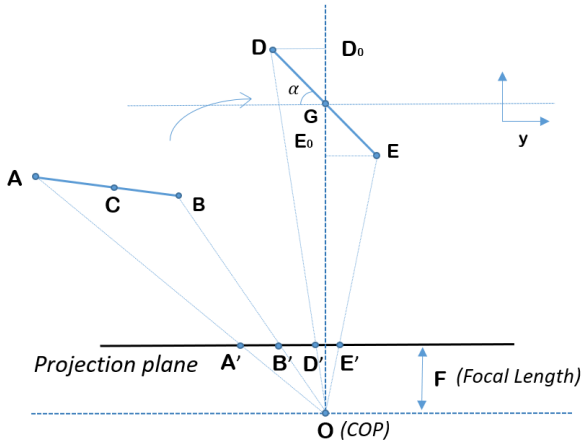

FIGURE 4. Non-centred line segment.

A. PROJECTIVE ROTATION IN 2D

Projective rotation provides direct relationship between the projected points before and after rotation.

Let A', B' represent the projection of the target segment bounded by A and B, and C' the projection of its mid-point C on the image plane. Let D', E' represent the projection of the target segment bounded by D and E, and G' represent

the projection of its mid-point G on the image plane. After rotation, the centre C of the real segment should be coincident with focal axis, and its projection is coincident with the centre the of image.

Since after rotation the angles between the three projected points do not change, the new projections after rotation can be derived after calculating the angles between the vectors $\vec{OA'}$, $\vec{OC'}$ and $\vec{OB'}$. If we let $\alpha_{A'C'}$ to be the angle $\angle(\vec{OA'}, \vec{OC'})$ and $\alpha_{B'C'}$ to represent the angle $\angle(\vec{OB'}, \vec{OC'})$, since these angles remain the same after rotation, the new projections y'_D and y'_E are derived in (8) and (9) where E', G' and D' are the new projected points respectively, and after rotation.

$$y_{D'} = F \cdot \tan(\alpha_{A'C'}) \tag{8}$$

$$y_{E'} = F \cdot \tan(\alpha_{B'C'}) \tag{9}$$

We note here that y'_D and y'_E can also be written as in (10) and (11):

$$y_{D'} = F^2 \cdot \frac{y_{A'} - y_{C'}}{F^2 + y_{A'} \cdot y_{C'}} \tag{10}$$

$$y_{E'} = F^2 \cdot \frac{y_{B'} - y_{C'}}{F^2 + y_{B'} \cdot y_{C'}} \tag{11}$$

Proof: Let $\alpha_{A'C'}$ be the angle $\angle(\vec{OA'}, \vec{OC'})$ then $\alpha_{A'C'} = \alpha_{D'} = \alpha_{A'} - \alpha_{C'}$ (after rotation). Or $\alpha_{c'} = (\alpha_{A'} + \alpha_{B'})/2$ where $\alpha_{A'} = \arctan(y_{A'}/F)$ and $\alpha_{B'} = \arctan(y_{B'}/F)$. This gives the following:

$$\begin{aligned}\alpha_{D'} &= \alpha_{A'} - \alpha_{C'} \\ &= \arctan(\frac{y_{A'}}{F}) - \arctan(\frac{y_{C'}}{F}) \\ &= \arctan\left(\frac{y_{A'} - y_{C'}}{F + y_{A'} \cdot y_{C'}}\right)\end{aligned}$$

which leads to

$$y_{D'} = F^2 \cdot \frac{y_{A'} - y_{C'}}{F^2 + y_{A'} \cdot y_{C'}}$$

□

B. DISTORTION FACTOR

Like before, we define the distortion factor to be the ratio of the projected length over the real length of the segment and we denote this factor by the small μ as in (12), but this time we append the letter T to distinguish between the total distortion factor and what we calculated before. Noting here that μ_T belongs to [0, 1].

$$\mu_T = \frac{|y_{B'} - y_{A'}|}{L} \qquad \mu_T \in [0 \quad 1] \tag{12}$$

C. FORESHORTENING DISTORTION FACTOR

Since the segment is not centred with respect to the focal axis, an additional factor is being added to μ_T. Let $|y_{A'} - y_{B'}|$ to be the projected length of the segment. The projected distance can also be written as a function of the projected length $|y_{D'} - y_{E'}|$ after applying a projective rotation as in equation (13).

This leads to the equation (14) where μ_T can be written in terms of pose and distance factor, and an additional factor that we call here foreshortening distortion factor (FDP). We denote the last factor by μ_3. Finally, we can put all the distortion factors in one equation, as in (15).

$$\underbrace{[y_{A'} - y_{B'}]}_{\text{projected length}} = [y_{D'} - y_{E'}] \cdot \frac{[F^2 + y_{C'} \cdot y_{A'}] \cdot [F^2 + y_{C'} \cdot y_{B'}]}{F^2 \cdot [F^2 + y_{C'}^2]} \tag{13}$$

$$\underbrace{\mu_T}_{\substack{\text{total distortion} \\ \text{factor}}} = \underbrace{\mu}_{\substack{\text{pose and distance} \\ \text{factor}}} \cdot \underbrace{\frac{[F^2 + y_{C'} \cdot y_{A'}] \cdot [F^2 + y_{C'} \cdot y_{B'}]}{F^2 \cdot [F^2 + y_{C'}^2]}}_{\text{foreshortening distortion factor}} \tag{14}$$

$$\underbrace{\mu_T}_{\text{TDF}} = \underbrace{\mu_1}_{\text{DDF}} \cdot \overbrace{\mu_2}^{\text{PDF}} \cdot \underbrace{\mu_3}_{\text{FDF}} \tag{15}$$

Proof: From (10) and (11), $y_{D'} - y_{E'}$ can be written as follows:

$$y_{D'} - y_{E'} = F^2 \cdot \frac{[F^2 + Y_{c'}^2] \cdot [Y_{A'} - Y_{B'}]}{[F^2 + y_{C'} y_{A'}] \cdot [F^2 + y_{C'} y_{A'}]}$$

which implies

$$y_{A'} - y_{B'} = [y_{D'} - y_{E'}] \cdot \frac{[F^2 + y_{C'} \cdot y_{A'}] \cdot [F^2 + y_{C'} \cdot y_{B'}]}{F^2 \cdot [F^2 + y_{C'}^2]}$$

□

Equation (14) tells us that if the segment is centred with respect to the focal axis, $y_{C'}$ is equal to 0 and the foreshortening factor becomes equal to 1.

In this section, we presented a detailed analysis of how distortion is being propagated and come up with a model of the total distortion on distances between two points when projected into the image plane. Since a line-segment form is the basis of every structure, it was very important to understand and model these distortions before proceeding in building the concept.

D. PROJECTIVE ROTATION IN 3D

Performing a 2D projective rotation to a projected point in the (XY) plane, has a direct impact on the coordinate of that projected point in the (ZX) plane. The unusual change in the Z-coordinates of the projected point after rotation is hard to be visualized from one plane. Figure 5(a) depicts the rotation in the (XY) plane, while in Figure 5(b) we show its impact from the (ZX) perspective. We point out at the points A and B, after rotation, by the points D and E respectively. We show here that when we rotate in one plane (XY), the corresponding z-coordinate of the projected point, after rotation, decreases as we rotate towards the centre. This is because the z-coordinate of the points A and B, does not change after rotation around the Z-axis. Only the X and Y-coordinates change.

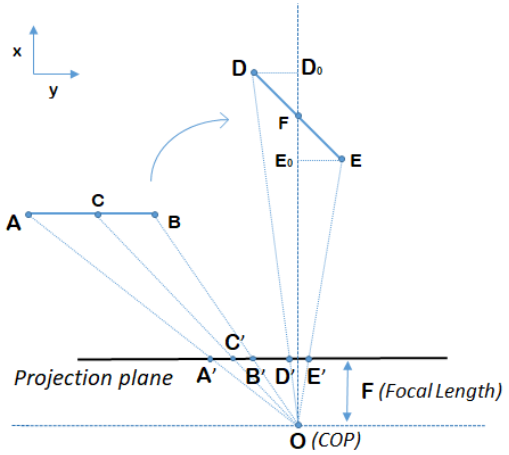

(a) Rotation in the (XY) plane.

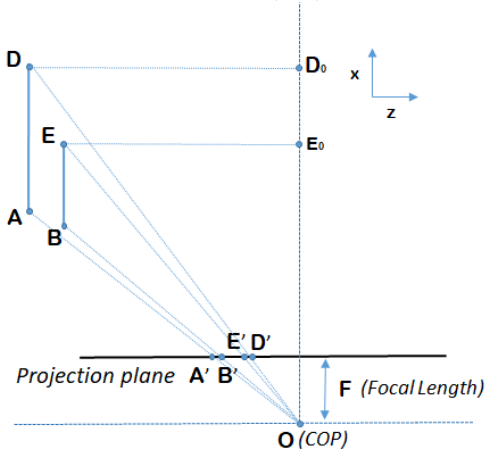

(b) Rotation impact on the z-coord. of the projected points seen from the (ZX) plane.

FIGURE 5. Projective rotation seen from the (XY) and (ZX) plane.

To calculate the z-coordinate of the projected point, after rotation, we use an intermediate point denoted D_1, as shown in figure 6. D_1 is the rotation of A' around the Z-axis. Since we are dealing with perspective projection, the Z-coordinate of the projection of the point D_1 is the same as the Z-coordinate of the projection of D, as in figure 6. Furthermore, we already calculated the Y-coordinate of D' from (10). The 2D coordinates of D_1 are written below as in (16).

$$D_1 = \begin{bmatrix} x_{D_1} \\ y_{D_1} \\ z_{D_1} \end{bmatrix} = \begin{bmatrix} A'O \cdot cos(\alpha) \\ A'O \cdot sin(\alpha) \\ z_{A'} \end{bmatrix} \tag{16}$$

The vector representation and derivation of D' is shown in (17),

$$D' = \begin{bmatrix} \frac{x_{D_1}}{x_{D_1}} \cdot F \\ \frac{y_{D_1}}{x_{D_1}} \cdot F \\ \frac{z_{D_1}}{x_{D_1}} \cdot F \end{bmatrix} = \begin{bmatrix} F \\ y_{D'} \\ \frac{z_{D_1}}{x_{D_1}} \cdot F \end{bmatrix} = \begin{bmatrix} F \\ F^2 \cdot \frac{y_{A'} - y_{C'}}{F^2 + y_{A'} \cdot y_{C'}} \\ \frac{z_{A'}}{A'O \cdot cos(\alpha)} \cdot F \end{bmatrix} \tag{17}$$

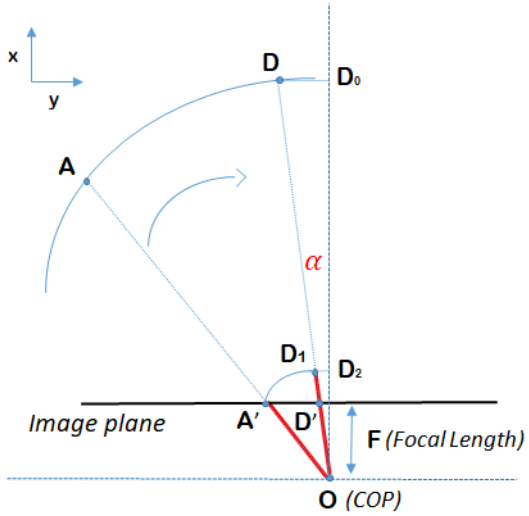

FIGURE 6. Derivation of the of the Z-coordinate from the (XY) plane.

and the Z-coordinate of D' can be obtained from (18) where we showed its derivation after rotation in (17).

$$z_{D'} = \frac{z_{A'}}{A'O \cdot cos(\alpha)} \cdot F \tag{18}$$

By deriving (10), (11) and (18), we have established a relationship between the projections of the points in space before and after rotation. These are fundamental equations to perform any projective rotation.

From these equations as well, we can derive the distance to the segment centre prior and after rotation by substituting (8) and (9) in (1) and (2) respectively. Knowing that $x_{center} = (x_D + x_E)/2$, x_{center} can be treated as the distance to the centre of the segment in case the rotation is with respect to the centre. Its derivation is depicted in (19).

$$x_{centre} = \frac{L \cdot F^2}{4} \cdot \left[\frac{y_{D'} - y_{E'}}{y_{D'} \cdot y_{E'}} \right] \cdot \cos(\alpha) \tag{19}$$

The tilted angle α can also be calculated from (4) and by adding to it the angle of rotation α_c it yields to (20).

$$\alpha = \arctan\left(\frac{F}{2} . \frac{y_{B'} + y_{A'}}{y_{A'} . y_{B'}} \right) + \alpha_c \tag{20}$$

IV. FORSHORETENING CORRECTION

Understanding and modelling perspective distortion is essential to eliminate this kind of distortion in image measurements for the distance between two points in space. The first step is to eliminate the foreshortening error, which is required to perform projective rotation to the segment relative to its centre. This will make the segment appear as if, in reality, it stands in the middle of the image and at the middle of the field of view. Performing a projective rotation requires the knowledge of the coordinates of a projected third point, which is ideally the projection of the mid-point of the line segment. Since the projection of the centre of the target in most cases is not known, a distinction between different rotation processes

is considered in order to select the proper rotation starting point. These processes are depicted below: (1)

1) Rotation from the target centre. This requires that the mid-point of the target to be known.
2) Rotation from the mid-point of the projected target.
3) Rotation from the mid-arc of the projection.

In all of the above three cases listed, the rotation is considered to happen around the $Z-axis$ when working in the (XY) plane, and around the $Y-axis$ when working in the (XZ) plane. Furthermore, cases (2) and (3) can be seen as complementary cases since they solve the same issue but one can have preferences in some occasions, as we will explore in the next section.

A. TARGET CENTRE LOCATION

It is important to picture where that centre could be, in order to perform a proper rotation that could totally eliminate the foreshortening distortion.

Considering a line segment $[AB]$ of a length L, Figure 7 shows that for any particular projection $[A'B']$, different position of the same segment $[AB]$ can be originated. All the segments in this figure are of the same length l but what can be noticed is that every possible unique position has a different tilted angle α. α is the angle formed by the segment and its projection, which lies on the image plane. This unique position of every segment depends on the angle α.

Finally, we rendered a plot, shown in Figure 7, of the position of all the centres of the segments' location curve.

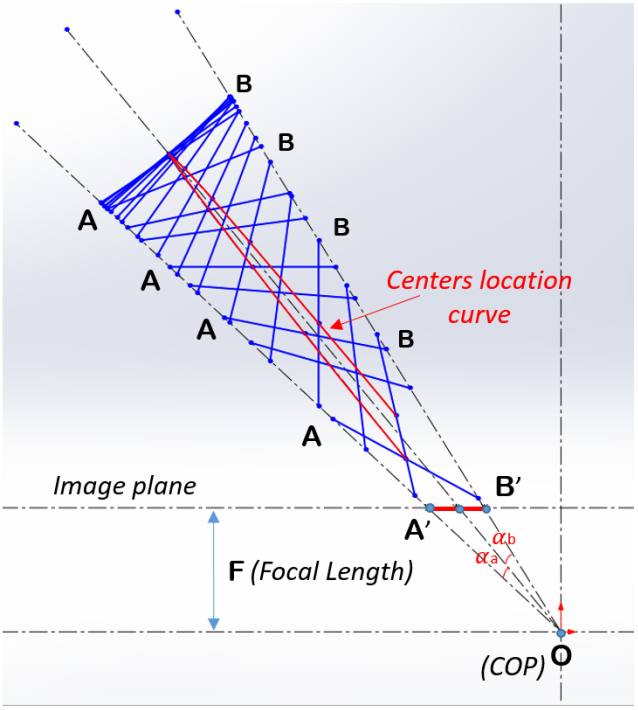

FIGURE 7. Possible location of the segment having the same projection in the image. The curve in red depicts the location of centres of all the segments.

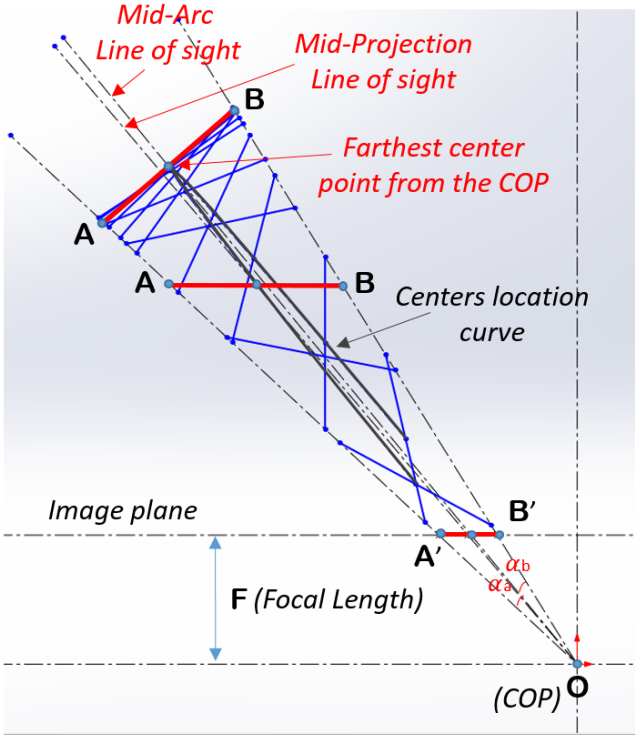

FIGURE 8. The figure shows the remarkable features extracted from the centre location curve. (1) the Mid-Arc axis is coincident with the Farthest centre possible. (2) The Mid-Projection axis is coincident with the segment that is parallel to the image plane.

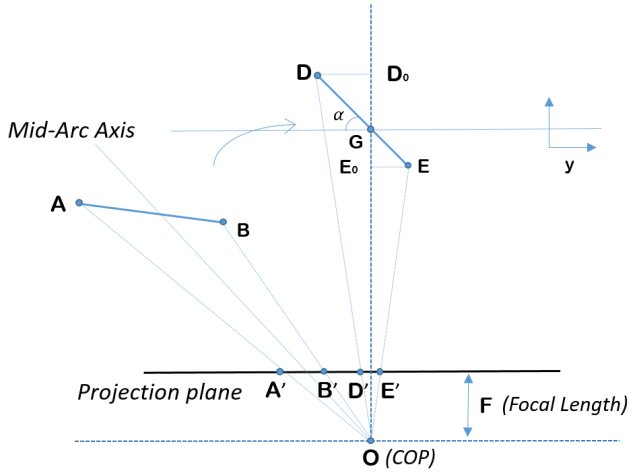

FIGURE 9. The figure shows the rotation from the Mid-Arc around the z-axis towards the centre. The Mid-Arc will be coincident with the focal axis after rotation.

The centre location curve has the shape of a parabola and has the line of sight as the axes of symmetry. What we noticed are some very notable features. There are two remarkable and important features, depicted in Figure 9, that can be extracted from this pattern. In this context, these remarkable features are referred to as aspect (1) and aspect (2).

1) **Aspect (1)**:The first distinctive feature is at the maximum of the centre location curve. This centre corresponds to the farthest possible segment from the

centre of projection. This segment represented by $[AB]$ is perpendicular to the mid-arc line of projection and it is the only segment at which its mid-point is coincident with the mid-arc line, as it is shown by the centres location curve in the Figure 9. This implies that the projection of its centre is also coincident with mid-arc line.

2) **Aspect (2)**:Another remarkable aspect is in the segment that is parallel to the image plane, with α equal to zero. This segment $[AB]$ has its mid-point coincident with the axis that intersects with the mid-point of the projected segment $[A'B']$ and the COP.

These are two important observations that represent how circular and spherical targets are projected into the image plane and can be used to establishing the concept of eccentricity elimination. Circular and spherical targets are not covered in this paper.

B. CENTRE LOCATION CURVE

When mid-arc rotation towards the centre is performed, the function of the centre location curve becomes centred and can be expressed by two parametric equations (21) and (22), with the angle α as the intermediate parameter. We plot these parametric equations, as shown in Figure 10.

$$x_c = \frac{L \cdot F}{2 \cdot y_{A'}} \cdot \cos(\alpha) \tag{21}$$

$$y_c = \frac{L \cdot y_{A'}}{2 \cdot F} \cdot \sin(\alpha) \tag{22}$$

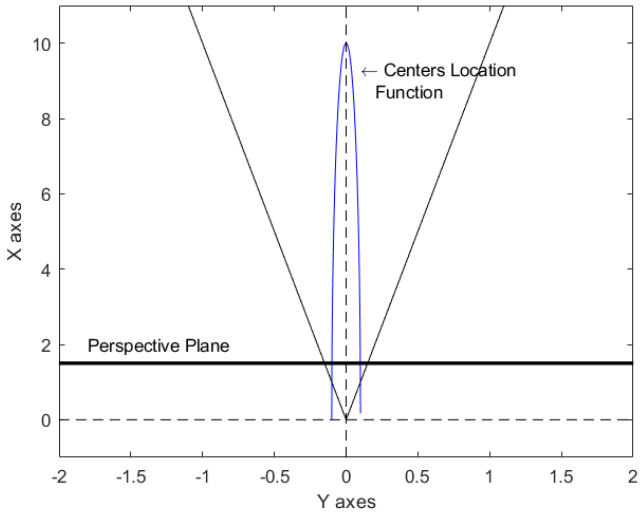

FIGURE 10. Centres location function after mid-arc rotation.

Proof: looking at Figure 10, let $x_{centre} = (x_D + x_E)/2$, and let G, which is not necessarily aligned with the focal axis, to represent the point of intersection of the segment $[DE]$ with the centre line of projection, then x_D and x_E can be expressed as follows,

$$x_D = \frac{F \cdot y_D}{y_{D'}} \cdot DG \cdot \cos(\alpha)$$

$$x_E = -\frac{F \cdot y_E}{y_{E'}} \cdot EG \cdot \cos(\alpha)$$

where $y_{D'}$ and $y_{E'}$ are the Y-coordinates of the corresponding projections of y_D and y_E on the projective plane. Since the rotation is a mid-arc rotation $y_{D'} = y_{E'}$, this yields to the X-coordinate of the centre of the segment as in (21). The same can be applied to determine the Y-coordinate of the centre. Let $y_{centre} = (y_D + y_E)/2$, substituting with y_D and y_E from the equations x_D and x_E which yields to (22). □

x_{centre} and y_{centre} here represent the coordinates of the centre where α is the angle formed by the perspective plane and the line-segment $[AB]$.

If now the rotation happens starting from the mid-point of the projection, the x-coordinate of the centre, derived from the location curve can be expressed by Equation (23).

$$x_c = \frac{F}{2} \cdot \left(\frac{DG}{y_{D'}} + \frac{EG}{y_{E'}}\right) \cdot \cos(\alpha) \tag{23}$$

C. LOCATING THE CENTRE FROM THREE POINTS

We have shown in the previous section that two points are not enough to locate the centre of the segment. In this section, we will show the derivation of the full pose from three points.

We have derived previously the parametric equations that define the centres location. Since the tilted angle α is not known, a third point is required to add one more constraint on the centre location curve parametric equations. This equation is depicted in (25).

$$x_c + d\sin(\alpha) = \frac{F}{y_{d'}}\left[y_c + d\cos(\alpha)\right] \tag{24}$$

Proof: Considering a third point D located at distance d from the centre C on the line segment, which derived by performing a mid-arc rotation as shown in Figure 11.

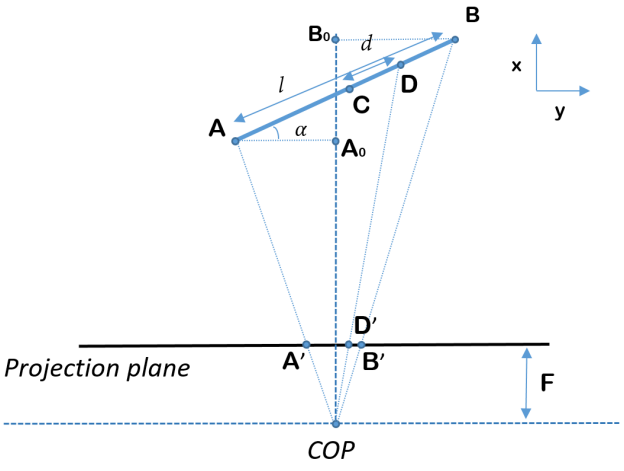

FIGURE 11. Locating the centre from three points on the segment after Mid-Arc rotation.

The equations that relate the point D to the centre are illustrated below.

$$\begin{cases} x_d - x_c = d\cos(\alpha) \\ y_d - y_d = d\sin(\alpha) \end{cases} \Longrightarrow \begin{cases} x_d = x_c + d\cos(\alpha) \\ y_d = y_d + d\sin(\alpha) \end{cases}$$

However, we can write the equation of the projected line from the point D as follows:

$$\begin{aligned} x_d &= a y_d \\ x_{d'} &= a y_{d'} \end{aligned} \Longrightarrow \quad a = \frac{F}{y_{d'}}$$

This leads to the additional constraint equation:

$$x_c + d\sin(\alpha) = \frac{F}{y_{d'}}\left[y_c + d\cos(\alpha)\right]$$

□

The system of equations become as in (25)

$$\begin{cases} x_c = \dfrac{L \cdot F}{2 \cdot y_{A'}} \cdot \cos(\alpha) \\ y_c = \dfrac{L \cdot y_{A'}}{2 \cdot F} \cdot \sin(\alpha) \\ x_c + d\sin(\alpha) = \dfrac{F}{y_{d'}}\left[y_c + d\cos(\alpha)\right] \end{cases} \tag{25}$$

From these equations we can extract the angle by replacing equation one and two into the third one in order to get Equation (26). Using (26) we can recalculate the coordinates of the centre x_c and y_c.

$$\alpha = \arctan\left(\frac{\frac{L \cdot F}{2 \cdot y_{A'}} - \frac{F}{y_{D'}} d}{\frac{F}{y_{D'}} \cdot \frac{L \cdot y_{A'}}{2 \cdot F} - d}\right) \qquad \alpha \in [-\frac{\pi}{2} \ \ \frac{\pi}{2}] \tag{26}$$

D. ELIMINATING THE FORESHORTENING ERROR

We have shown previously that the projective rotation requires the knowledge of the centre. Knowing the centre allows to perform a rotation towards the centre and to eliminate the eccentric error. After rotation from the centre, $y_{c'}$ becomes equal to 0. This makes the FDF to become equal to 1, meaning that its effect has no impact on the projected distance, regardless of the distance and pose of the segment. On the other hand, when the centre is not known, the foreshortening effect can never be fully recovered but at a certain extent, depending on the pose of the segment.

V. POSE AND DISTANCE CORRECTION

The pose and distance factor depend on the angle formed by the segment and its projection into the image plane, and of the distance of the target with respect to the COP. These two parameters are fundamental in correcting image measurements from the distorted projection of the target in the image.

Compensating for the pose effect and evaluating the pose factor requires that the tilted angle α to be cognised or calculated. In most cases, the derivation of the angle α requires the knowledge of a third point as we showed previously. While knowing the real length l of the segment, constraints on the distance estimation equations can be imposed, reducing the number of solutions into close form solution. This type of constraints are know as geometric constraints and are used in various applications in photogrammetry and Marker-Based pose estimation.

VI. CONCLUSION

In this paper, we modeled perspective distortion in all of its forms. We elaborated on the importance of understanding how shapes are projected into the image in order to improve image measurements. We went deeply into every aspect of perspective distortion by deriving all the equations that form the basic building blocks of distance measurements. The resulted equations showed an analogy of how shapes appear distorted in images. Furthermore, we provided ways for evaluating and correcting image measurements induced by these kinds of distortions. We were also able to show how these distortions could be eliminated, based on the cases and the number of points known, as discussed.

In some cases, the reversed problem matters where the interest is to locate the segment in space and only the projected distances onto the perspective plane or image plane are known. It is then relevant to clear out the distortions which makes it possible; for example, to calculate accurately the position and orientation of the target object with respect to the COP. This same approach can be extended to evaluate the distortion on different target shapes for the purpose of improving image measurements of the object within the scene, by knowing only the projected geometry onto the perspective plane.

The work can be extended to different geometry models. Since line-segments form the basis of every structure, it was very important to elaborate and model these distortions on a simple geometry before proceeding to studying more complex forms. Although line segments can be useful for the demonstrations and evaluations, it is very likely in real life to fall into a singularity. This is the case where both edges of the segment are coincident with the focal axis. This is due to a major fact provided by the natural property, which is co-linearity of points located on the line. Co-linearity provokes the system to lose a degree of freedom. Because of this, more geometric constraints are needed, like non co-linear target geometry in order to avoid for the system to return into infinite solutions. Fortunately, circular and spherical targets have similar properties when it comes to projection into the image plane.

REFERENCES

[1] B. Peng, W. Wang, J. Dong, and T. Tan, "Position determines perspective: Investigating perspective distortion for image forensics of faces," in *Proc. IEEE Conf. Comput. Vis. Pattern Recognit. Workshops (CVPRW)*, Jul. 2017, pp. 1813–1821.

[2] P. Corke, *Robotics, Vision and Control: Fundamental Algorithms in MATLAB*, 1st ed. Springer, 2013.

[3] A. Bousaid, T. Theodoridis, and S. Nefti-Meziani, "Introducing a novel marker-based geometry model in monocular vision," in *Proc. 13th Workshop Positioning, Navigat. Commun. (WPNC)*, Oct. 2016, pp. 1–6.

[4] A. Y. Brailov, *Engineering Graphics: Theoretical Foundations of Engineering Geometry for Design*, 1st ed. Springer, 2016.

[5] Z. Tang, R. Grompone Von Gioi, P. Monasse, and J.-M. Morel, "A precision analysis of camera distortion models," *IEEE Trans. Image Process.*, vol. 26, no. 6, pp. 2694–2704, Jun. 2017.
[6] J. G. Fryer, "Lens distortion for close-range photogrammetry," *Photogramm. Eng. Remote Sens.*, vol. 52, no. 1, pp. 51–58, 1986.
[7] T.-Y. Lee, T.-S. Chang, and S.-H. Lai, "Correcting radial and perspective distortion by using face shape information," in *Proc. 11th IEEE Int. Conf. Workshops Autom. Face Gesture Recognit. (FG)*, vol. 1, May 2015, pp. 1–8.
[8] C. Ricolfe-Viala and A.-J. Sanchez-Salmeron, "Lens distortion models evaluation," *Appl. Opt.*, vol. 49, no. 30, p. 5914, Oct. 2010.
[9] X. Wang and R. Klette. (Apr. 2005). *Geometric Correction of Projected Rectangular Pictures*. [Online]. Available: http://citr.auckland.ac.nz/techreports/2005/CITR-TR-167.pdf
[10] Z. Wang, H. Liang, X. Wu, Y. Zhao, B. Cai, C. Tao, Z. Zhang, Y. Wang, S. Li, F. Huang, S. Fu, and F. Zhang, "A practical distortion correcting method from fisheye image to perspective projection image," in *Proc. IEEE Int. Conf. Inf. Autom.*, Aug. 2015, pp. 1178–1183.
[11] M. Feng, B. Fang, and W. Yang, "Fast reducing perspective distortion for road marking recognition," in *Proc. IEEE 20th Int. Conf. Intell. Transp. Syst. (ITSC)*, Oct. 2017, pp. 1–6.
[12] O. Arandjelovic, D.-S. Pham, and S. Venkatesh, "CCTV scene perspective distortion estimation from low-level motion features," *IEEE Trans. Circuits Syst. Video Technol.*, vol. 26, no. 5, pp. 939–949, May 2016.
[13] J. Valente and S. Soatto, "Perspective distortion modeling, learning and compensation," in *Proc. IEEE Conf. Comput. Vis. Pattern Recognit. Workshops (CVPRW)*, Jun. 2015, pp. 9–16.
[14] L. Li and C. L. Tan, "Character recognition under severe perspective distortion," in *Proc. 19th Int. Conf. Pattern Recognit.*, Dec. 2008, pp. 1–4.
[15] Y. Wang, Y. Sun, and C. Liu, "Layout and perspective distortion independent recognition of captured chinese document image," in *Proc. 14th IAPR Int. Conf. Document Anal. Recognit. (ICDAR)*, vol. 1, Nov. 2017, pp. 591–596.
[16] M. A. Fischler and R. C. Bolles, "Random sample consensus: A paradigm for model fitting with applications to image analysis and automated cartography," *Commun. ACM*, vol. 24, no. 6, pp. 381–395, Jun. 1981.
[17] B. Lee, K. Daniilidis, and D. D. Lee, "Online self-supervised monocular visual odometry for ground vehicles," in *Proc. IEEE Int. Conf. Robot. Autom. (ICRA)*, May 2015, pp. 5232–5238.
[18] X.-S. Gao, X.-R. Hou, J. Tang, and H.-F. Cheng, "Complete solution classification for the perspective-three-point problem," *IEEE Trans. Pattern Anal. Mach. Intell.*, vol. 25, no. 8, pp. 930–943, Aug. 2003.
[19] J. Y. Aloimonos, "Perspective approximations," *Image Vis. Comput.*, vol. 8, no. 3, pp. 179–192, Aug. 1990, doi: 10.1016/0262-8856(90)90064-c.
[20] T. Luhmann, "Eccentricity in images of circular and spherical targets and its impact to 3D object reconstruction," *Int. Arch. Photogramm. Remote Sens. Spatial Inf. Sci.*, vol. 45, pp. 363–370, Jun. 2014.
[21] M. Neumann, E. Breton, L. Cuvillon, L. Pan, C. H. Lorenz, and M. De Mathelin, "Evaluation of an image-based tracking workflow using a passive marker and resonant micro-coil fiducials for automatic image plane alignment in interventional MRI," in *Proc. Annu. Int. Conf. IEEE Eng. Med. Biol. Soc.*, Aug. 2012.
[22] R. Matsuoka and S. Maruyama, "Eccentricity on an image caused by projection of a circle and a sphere," *ISPRS Ann. Photogramm. Remote Sens. Spatial Inf. Sci.*, vol. 3, pp. 19–26, Jun. 2016.
[23] T. Luhmann, "Eccentricity in images of circular and spherical targets and its impact on spatial intersection," *Photogramm. Rec.*, vol. 29, no. 148, pp. 417–433, Dec. 2014.
[24] S. Yang, J. Liu, W. Yang, and Z. Guo, "Perspective distorted video restoration and stabilization for mobile devices," in *Proc. IEEE China Summit Int. Conf. Signal Inf. Process. (ChinaSIP)*, Jul. 2015, pp. 423–427.
[25] M. A. Tehrani, A. Majumder, and M. Gopi, "Correcting perceived perspective distortions using object specific planar transformations," in *Proc. IEEE Int. Conf. Comput. Photogr. (ICCP)*, May 2016, pp. 1–10.
[26] Y. Takezawa, M. Hasegawa, and S. Tabbone, "Camera-captured document image perspective distortion correction using vanishing point detection based on Radon transform," in *Proc. 23rd Int. Conf. Pattern Recognit. (ICPR)*, Dec. 2016, pp. 3968–3974.
[27] X. Cui, Y. Zhao, K. Lim, and T. Wu, "Perspective projection model for prism-based stereovision," *Opt. Express*, vol. 23, no. 21, pp. 27542–27557, Oct. 2015.
[28] T. D'Orazio, N. Ancona, G. Cicirelli, and M. Nitti, "A ball detection algorithm for real soccer image sequences," in *Proc. Object Recognit. User Interaction Service Robots*, Jun. 2003, pp. 210–213.
[29] F. Liu, C. Shen, G. Lin, and I. Reid, "Learning depth from single monocular images using deep convolutional neural fields," *IEEE Trans. Pattern Anal. Mach. Intell.*, vol. 38, no. 10, pp. 2024–2039, Oct. 2016.
[30] A. Saxena, S. H. Chung, and A. Y. Ng, "Learning depth from single monocular images," in *Proc. Adv. Neural Inf. Process. Syst.*, 2006, pp. 1161–1168.
[31] N. K. Kottayil, I. Cheng, G. Valenzise, and F. Dufaux, "Learning local distortion visibility from image quality," in *Proc. 25th IEEE Int. Conf. Image Process. (ICIP)*, Oct. 2018.
[32] A. Soycan and M. Soycan, "Perspective correction of building facade images for architectural applications," *Eng. Sci. Technol., Int. J.*, vol. 22, no. 3, pp. 697–705, Jun. 2019. [Online]. Available: http://www.sciencedirect.com/science/article/pii/S2215098618314137

ALEXANDRE BOUSAID was born in Beirut, Lebanon, and Pays des Cèdres, centre of the Middle-East, where he grew up in a nature-lover family. He received the B.E. degree in computer and communication engineering and the M.S. degree in robotics and industrial engineering from the Holy Spirit University of Kaslik, in 2012, and the Ph.D. degree in robotics from the University of Salford, Manchester, in 2015, after being awarded the MSCA (Marie Skłdodowska-Curie Actions) research fellowship. His undergraduate years come to sharp focus on embedded systems and computer vision, working in global leading companies. His research interest includes vision-based systems and fundamentals of pose estimation, where he developed his own pose estimation method for mobile robotics.

THEODOROS THEODORIDIS received the Ph.D. degree in crime recognition surveillance robots from the University of Essex, U.K. He worked as a Postdoctoral Research Officer (EPSRC grand) on multimodal human–robot interfaces, visual guidance, and pattern recognition control methods with NASA Jet Propulsion Laboratory (JPL). He is currently working as an Associate Professor (Reader) leading a role in robotics and intelligent systems with the School of Science Engineering and Environment, Salford University, Manchester, U.K. He has been an Investigator of several national and European research grants attracting significant funding as a PI: £43K and a Co-I: £14M, totaling a grant income of £850K in successful bids, and delivered many research initiatives in application areas, including nuclear, healthcare, and robotics (EU FP5-7 for R&I, EPSRC, MRC, RGF, CST RDF, Innovate UK, and BBC RDF-TV). He is also an Honorary Visiting Professor in mechatronics with Manipal University, Dubai, and the Inventor of the home service robot Carebot. He is also a Reviewer and the author of several leading journals of the field, such as the IEEE TRANSACTIONS ON SYSTEMS, MAN AND CYBERNETICS, *Human-Machine Systems*, and *Evolutionary Computation*.

SAMIA NEFTI-MEZIANI is currently the Chair of artificial intelligence and robotics and the Director of the Centre for Autonomous Systems and Advanced Robotics, University of Salford. She has a well-established track record and has published extensively in the areas of advanced robotics systems and the development of artificial cognitive models for robotic systems. She is also the Coordinator of the Marie Curie ITN in advanced robotics, SMART-E, and the Coordinator and CO-I of three further major national programs in autonomous systems and robotics funded by the National Research Council and the technology strategy board worth more than €14M and was involved in the FP6 and FP7 research programs, such as Robotcup and NovelQ. She is a member of advisory board of the U.K. Research Council EPSRC Centre. She is also the Director of international industrial sponsored postgraduate programs in robotics. She is also the Vice Chairman of the IEEE Robotics and Automation U.K. and RI and an Associate Editor of the IEEE TRANSACTIONS ON FUZZY SYSTEMS. She is also one of the Founders of the Northern U.K. Robotics and Autonomous Systems Network.

STEVE DAVIS received the Ph.D. degree in advanced robotics from the University of Salford, U.K., in 2005. He became the Team Leader with the Italian Institute of Technology, in 2008. He is currently the Chair of advanced robotics with the University of Salford. His research interests include manufacturing, lightweight advanced actuators and artificial muscles, soft robotics, human–robot interaction, dexterous robot hands, biomimetics and biologically inspired robot systems, and robotics in healthcare and rehabilitation. He has published extensively on soft robotics, biomimetics, grippers and humanoid technologies, and automation. He has guest edited journals and been on the programme committee for many IEEE conferences, including and has attracted significant research funding both nationally and at a European level.